ADVANCED FUNCTIONAL MATERIALS
www.afm-journal.de

Encapsulating Elastically Stretchable Neural Interfaces: Yield, Resolution, and Recording/Stimulation of Neural Activity

Oliver Graudejus, Barclay Morrison III, Cezar Goletiani, Zhe Yu, and Sigurd Wagner*

A high-resolution elastically stretchable microelectrode array (SMEA) for interfacing with neural tissue is described. The SMEA consists of an elastomeric substrate, such as poly(dimethylsiloxane) (PDMS), elastically stretchable gold conductors, and an electrically insulating encapsulating layer in which contact holes are opened. We demonstrate the feasibility of producing contact holes with 40 μm × 40 μm openings, show why the adhesion of the encapsulation layer to the substrate is weakened during contact hole fabrication, and provide remedies. These improvements result in greatly increased fabrication yield and reproducibility. An SMEA with 28 microelectrodes was fabricated. The contact holes (100 μm × 100 μm) in the encapsulation layer are only ~10% the size of the previous generation, allowing a larger number of microelectrodes per unit area, thus affording the capability to interface with a smaller neural population per electrode. This new SMEA is used to record spontaneous and evoked activity in organotypic hippocampal tissue slices at 0% strain before stretching, at 5% and 10% equibiaxial strain, and again at 0% strain after relaxation. Stimulus–response curves at each strain level are measured. The SMEA shows excellent biocompatibility for at least two weeks.

1. Introduction

Elastically stretchable conductors have great potential for applications in dielectric elastomer actuators (DEAs),[1] sensitive electronic skin,[2,3] interconnects for stretchable electronics,[4,5] and neural interfaces in biomedical engineering.[6–8] These elastically stretchable conductors consist of an elastomeric substrate, such as the silicone poly(dimethylsiloxane) (PDMS), and a microcracked gold film,[9,10] a buckled film,[11–13] copper meanders,[14] or embedded carbon nanotubes.[15] Most applications of stretchable conductors require their encapsulation for electrical insulation and mechanical protection. While the encapsulation layer is an important component in stretchable electronics applications, it has received relatively little attention in the literature.[7,10,16]

The focus of this article is the reliable fabrication of soft (Young's modulus ~2 MPa) and stretchable neural interfaces and their application for neural field potential recording and stimulation. Stiff and rigid microelectrodes have been used for decades for extracellular stimulation and recording of neural activity.[17,18] There are several advantages for neural interfaces based on soft, compliant, elastically stretchable materials compared to conventional materials. In vivo, the reduced mismatch in mechanical properties between the surrounding tissue and the microelectrode, as well as the compliance of the microelectrode, causes less inflammation and scar tissue formation.[19,20] In vitro, stretchable microelectrode arrays (SMEAs) allow the simultaneous application of mechanical and electrical stimuli to a tissue, while concurrently recording the tissue response. This is important for the study of neurotrauma, particularly traumatic brain injury.[6,10]

Major challenges of encapsulating stretchable neural interfaces are the biocompatibility of the encapsulating material, adhesion of the encapsulation layer to the substrate, and the capability to produce contact holes to the underlying conductor, which acts as an electrode. These contact holes need to be small enough to allow recording/stimulation of individual neurons or a small neural population. However, the noise of the recording and the charge density during stimulation of neural activity both increase with decreasing size of the contact hole. The ideal diameter of the contact hole therefore depends on the specific application, and is typically between 10 μm and 50 μm in commercial microelectrodes.[21] Five different methods are currently used to pattern PDMS encapsulation layers: i) laser ablation,[22] ii) wet etching,[23] iii) dry etching,[7,24] iv) casting,[14,16,25–28] and v) photopatterning an elastomeric photoresist.[10,29–31] For a more detailed review, see Schuettler et al.[32]

Prof. O. Graudejus
Department of Chemistry and Biochemistry
Center for Adaptive Neural Systems
Arizona State University
Tempe, AZ 85287, USA
E-mail: oliver.graudejus@asu.edu
Prof. B. Morrison III, Dr. C. Goletiani
Department of Biomedical Engineering
Columbia University
New York, NY 10027, USA
Prof. Z. Yu
Institute of Biomedical and Health Engineering
Shenzhen Institute of Advanced Technology
Chinese Academy of Sciences
1068 Xueyuan Avenue, Shenzhen University Town
Shenzhen, 518055, China
Prof. S. Wagner
Department of Electrical Engineering and Princeton Institute for the Science and Technology of Materials
Princeton University
Princeton, NJ 08544, USA

DOI: 10.1002/adfm.201102290

i) Laser ablation is the only patterning method that does not require photolithography, however, a powerful laser is required and the minimum attainable feature size is >100 μm.[32] The ablation process needs to be carefully optimized to avoid damaging the metal underneath the encapsulating PDMS. ii) Wet and iii) dry etching both require the deposition and patterning of a hard mask (typically aluminum) before etching and the removal of this hard mask after etching, adding complexity to the fabrication process. In the dry etch process, the PDMS is removed by reactive ion etch (RIE) in an oxygen plasma with a fluorine containing source gas, such as CF_4[7] or SF_6.[24] Neural interfaces with 60 μm wide electrodes[7] and square test structures with openings of 30 μm have been created using this approach.[24] However, the metal conductors (even Au and Pt) underneath the PDMS are also chemically attacked by the fluorine atoms in the plasma discharge, thus careful process optimization is required. Process complexity, small process window, attack of the metal conductor and long etch times are drawbacks of dry etching. In the wet etch process, the PDMS is removed in a solution of tetrabutylammonium fluoride ($N(C_4H_9)_4F$) in n-methyl-2-pyrrolidinone (C_5H_9NO).[23] Because the metal is not attacked by the etchant, the selectivity for etching PDMS over the metal is very high. However, the process complexity and the minimum attainable feature size of >100 μm due to the isotropic nature of the etching process are major drawbacks. iv) The process flow for patterning the encapsulation layer by casting is reversed from the methods mentioned above. A thick photoresist (e.g., SU-8) that serves as a mold is patterned first, followed by spin-on of the PDMS at a thickness that is lower than the height of the photoresist. The photoresist is stripped after curing of the PDMS. The process affords a high resolution and aspect ratio, and can be done reliably. It is therefore widely used in MEMS applications. Neural interfaces with <100 μm diameter microelectrodes have been fabricated using this technology.[16] However, this patterning method limits the thickness of the encapsulation layer to the thickness of the photoresist. Furthermore, some PDMS often sticks to the top of the photoresist and needs to be gently removed by swabbing before stripping the photoresist, which makes it challenging to pattern complex features.

v) Photopatterning contact holes directly in the encapsulation is conceptually similar to patterning a negative photoresist. In this method, a photosensitive catalyst in the pre-polymer is activated by UV exposure. The activated catalyst facilitates the crosslinking reaction in which a vinyl-terminated siloxane and a poly(methylhydro-siloxane) oligomer are coupled in a hydrosilylation reaction. The crosslinking reaction, i.e., the hardening of the pre-polymer, only occurs in the UV-exposed regions. The pre-polymer in the unexposed regions is not crosslinked (catalyst is not activated), thus remains soluble in the developer and can be rinsed off. The resulting pattern in the silicone is therefore equivalent to the one of a negative photoresist. The WL5000 series of photopatternable silicones (PPS) from Dow Corning[33] uses a Pt-catalyst to mediate the crosslinking. In another variety of this method, photosensitive compounds (2,2-dimethyl-2-phenyl acetophenone, DMAP, or 2-hydroxy-2-methylpropiophenone) are added to the pre-polymer mixture to impart photopatternability.[29] A positive image of the photomask is obtained by adding benzophenone as photoinhibitor.[29,31] In either variety, the processing sequence is similar to patterning a photoresist: spin on, soft-bake, exposure, hard-bake, development and cure. An advantage of this method is that only standard microfabrication equipment and procedures are required, allowing for excellent process control, high reliability and reproducibility, and low cost fabrication. The PPS WL5150 is commercially available and was demonstrated to be biocompatible in bioMEMS applications for at least 4 days.[30]

We adopted the method just described of photopatterning contact holes in the encapsulation. We already demonstrated the capability of SMEAs that were encapsulated with a PPS (WL5150 from Dow Corning) to record and stimulate neural activity from hippocampal tissue slices at equibiaxial strain of up to 13.3%.[6,10] The SMEAs in these previous experiments had 11 microelectrodes with 300 μm × 300 μm wide contact holes and an active electrode area of 200 μm × 100 μm. To interface with a small neural population and to significantly increase the number of electrodes that interface with the tissue (size: ~4 mm^2), contact holes and active electrode areas with a diameter of less than 100 μm are required. To achieve these goals, the resolution of the patterning process needs improvement. Another challenge is frequent delamination of the PPS from the substrate during the development process, which severely limits the fabrication yield.

The focus of this work is to improve the resolution and reliability of the encapsulation process, and to fabricate functional SMEAs using this new high resolution process. We first describe how the resolution of patterning contact holes in the encapsulation layer can be improved such that contact holes with as small as 40 μm diameter can be opened. We identify the factors that lead to delamination of the PPS from the PDMS, and we demonstrate how the adhesion, and therefore yield, can be improved. We then describe the fabrication of SMEAs with 28 microelectrodes and 100 μm openings. The contact holes have only ~10% the area of those previously reported. Finally, we use these SMEAs for neural field potential recording and stimulation over one complete cycle of stretching and relaxation, i.e., before stretching, at up to 10% equibiaxial strain, and after relaxation. Specifically, we demonstrate (a) how these SMEAs are applied to record spontaneous and evoked neural activity from a hippocampal tissue slice, (b) how the spontaneous activity, the peak shape of stimulated activity, and the stimulus/response (SR) curve from a hippocampal tissue slice change with strain on the SMEA (the tissue was not stretched appreciably), and (c) that the SMEAs are biocompatible for at least two weeks in vitro. **Table 1** compares dimensions and number counts of commercially available rigid microelectrode

Table 1. Comparison of commercially available rigid and flexible MEAs[21] with SMEAs presented in this work.

	rigid MEA	flexible MEA	stretchable MEA (SMEA)
substrate material	glass	polyimide	PDMS
number of recording electrodes	60/256	24/32/64	28
electrode diameter	10–30 μm	30–100 μm	40–100 μm
electrode spacing (center-to-center)	100–200 μm	300–700 μm	200 μm

arrays (MEAs) on glass[21] and flexible MEAs on polyimide[21] with the SMEAs presented in this work.

For clarity, we use the term "microelectrodes" when referring to the whole conductor, and the term "recording site" when referring to the portion of the microelectrode that is exposed by the contact hole in the PPS.

2. Results

The fabrication of SMEAs has been previously described.[10] In short, a PDMS membrane is spun on a glass slide and cured. A Cr/Au/Cr metal stack is deposited and the microelectrodes are patterned by lithography and wet etching. The encapsulation of the microelectrodes and the opening of contact holes are accomplished using a PPS.

2.1. Encapsulation with Photopatternable Silicone (PPS)

The PPS is essentially a negative elastomeric photoresist that remains on the sample after fabrication. The processing involves the following steps:

i) Exposure of the sample to an oxygen plasma: Enhancement of adhesion of PPS to PDMS.
ii) Spin-on of the PPS and soft bake for 2 minutes at 110 °C: Solvent evaporation.
iii) Exposure to broadband UV radiation: Conversion of the catalyst in the PPS to the active form.
iv) Hard bake at 150 °C: Crosslinking of the PPS by the active catalyst.
v) Development: Removal of PPS not crosslinked.

2.1.1. Resolution

To improve the resolution of the patterning process, we minimized (1) thermal and (2) photochemical activation of the catalyst in the contact holes, (3) improved the development process, and (4) evaluated reducing the thickness of the PPS.

2.1.1.1. Reduce Thermal Activation and Lateral Diffusion of the Catalyst During Hard Bake. The catalyst in the PPS can be activated photochemically (desired), and thermally (not desired). To achieve the best resolution, thermal activation of the catalyst must be avoided. There are two thermal treatment steps during processing of the PPS: (1) the soft bake (110 °C), which reduces the solvent content before exposure, and (2) the hard bake (150 °C) which produces the crosslinking in the PPS.

The duration of the soft bake step at 110 °C (2 min or 5 min) did not affect the resolution appreciably (data not shown), suggesting that a temperature of 110 °C is not sufficient to thermally crosslink the PPS. One advantage of a longer soft bake is the reduction of the tackiness of the PPS which eases subsequent handling.

The duration of the hard bake step at 150 °C did appreciably affect the resolution of patterning the PPS. To evaluate the maximum hard bake time before appreciable thermally induced crosslinking occurs, PPS was spun on three glass slides with the process described above, skipping the UV exposure, however. Photochemical catalyst activation is therefore negligible, and any PPS residue on the glass slide after development originates from thermal crosslinking only. Hard bake times of 120 s, 150 s and 180 s were evaluated (all at 150 °C). After development, interference fringes (data not shown) indicated that silicone residue covered a large part of the glass slide when the sample was hard baked for 180 s, but less so for 150 s. For a hard bake time of 120 s no silicone residue was observed. The effect of thermal crosslinking on the size of the "foot" at the bottom of a feature was evaluated by exposing half of the glass slide followed by hard bake for 120 s, 150 s, and 180 s: The longer the hard bake, the larger the "foot" (see Supporting Information). At 120 s hard bake time, the "foot" is small.[34]

To compare the resolution for different process conditions and hole sizes, we fabricated a photomask with square features ranging from 10 µm to 500 µm. **Figure 1** shows the residue in the contact hole after development (300 µm thick PDMS, and 1 mm thick glass plates). 180 s hard bake time causes significant thermal crosslinking in the contact hole, thereby deteriorating the resolution. However, even at 120 s hard bake time, the resolution of the patterning process is only 300–500 µm, which is insufficient for the intended application. Further reducing the hard bake time reduces adhesion of the PPS to the PDMS substrate.

2.1.1.2. Minimize Photochemical Activation of the Catalyst in Unexposed Areas. Reflection and scattering of photons into the contact holes can be greatly reduced by covering the (metallic, and therefore reflective) sample tray of the mask aligner with a black sheet or by coating the back of the glass slide with a poorly reflective coating (e.g., a 20–30 nm thick Cr film). Reducing reflection of UV light during exposure reduces the "foot" in the contact holes and thus improves the resolution (see Supporting Information). Figure 1 shows that the resolution of the patterning process can be improved to 50 µm by covering the sample tray with a black sheet and using a hard bake time of 120 s. **Figure 2**a shows the profilometer scans across 25 µm to 500 µm wide square contact holes. There is no residue in the contact hole with sides that are 50 µm or longer. A residue of about 4 µm of PPS remains in 25 µm square holes. A metal electrode at the bottom of this contact hole would be electrically insulated. Figure 2b shows Sscanning electron microscope (SEM) images of 25 µm, 50 µm and 100 µm wide square contact holes. The 50 µm and 100 µm wide features are well resolved. The 25 µm wide features are rounded.

2.1.1.3. Exposure Dose. The exposure dose for the PPS patterning was chosen to be (a) long enough to ensure complete crosslinking, and (b) not longer than necessary to avoid overexposure which increases the size of the foot, thus, reduces resolution. The PPS thickness after the hard bake step is 20–22 µm. This thickness is reduced during the development step as some PPS dissolves in the developer.[33] The thickness of the PPS after development is a strong function of the exposure time, i.e., of the extent of the crosslinking. For an exposure time of 60 s, the PPS thickness is about 7 µm, i.e., two thirds of the PPS was removed during the development. The PPS thickness increases with exposure time and reaches a maximum of 14–15 µm at an exposure time of 240 s, i.e., the PPS is completely cured. Increasing the exposure time beyond 240 s does not further

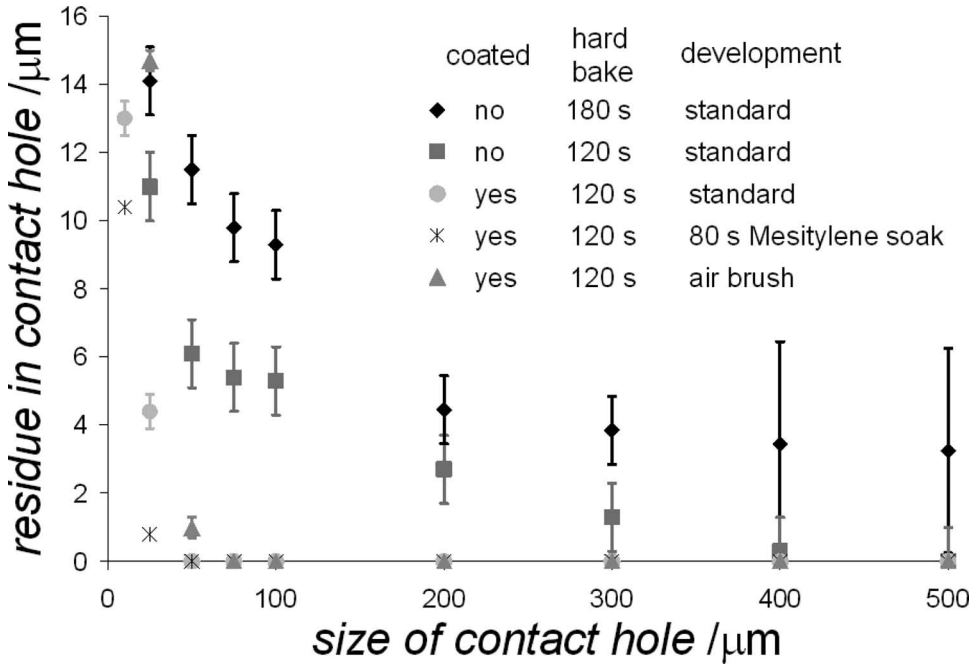

Figure 1. PPS residue in contact hole vs. the size of the square contact hole for different encapsulation processes: coated vs. not coated, hard bake times, and development.

increase the PPS thickness after development (see Supporting Information), but increases the size of the foot.

When glass slides or silicon wafers are used as substrates for PPS, even low exposure times (e.g., 60 s) provide well defined features with adhesion adequate for tolerating the development process. However, when PDMS is used as a substrate, underexposing often leads to complete delamination of the PPS during the development process. We therefore chose an exposure time of 300 s to ensure complete crosslinking and to provide a sufficient process window to allow for sample-to-sample variations.

2.1.1.4. Development. The resolution of the patterning process is strongly affected by the development method. The standard method for the development is to puddle soak the PPS in mesitylene (or Stoddard developer) for 40 s, then shower rinse the spinning sample with 100 mL isopropyl alcohol (IPA), this sequence being carried out twice.[33] On a PDMS substrate without microelectrodes, doubling the time of the mesitylene puddle soak in the first step of the development from 40 s to 80 s reduces the residue in the 25 μm contact holes from >4 μm to about 0.8 μm (see Figure 1). This potentially allows for an increased process margin for patterning 50 μm wide features.

We evaluated alternative development processes to eliminate or reduce the mechanical force, such as a mesitylene puddle followed by an IPA puddle, or an immersion-soak with up to 9 repetitions. The resolution of the patterning did greatly deteriorate compared to the standard process, and even 300 μm × 300 μm contact holes could not be fully opened (data not shown). This indicates that mechanical force is required to remove from the contact holes the WL5150 that is not crosslinked. Using an air-brush (≈30 psi pressure) instead of a shower rinse, allows to reliably produce 75 μm × 75 μm holes in the PPS (Figure 1).

2.1.1.5. PPS Thickness. The PPS has a sloped sidewall profile, thus, reducing the PPS thickness may improve the resolution. The PPS thickness was reduced by diluting the WL5150 with mesitylene, which is also the solvent in commercial PPS. The PPS thickness decreases with dilution and with increasing spin rate (see Supporting Information). However, striations, i.e., inhomogeneities, form in the film at 25 vol% and 50 vol% dilution regardless of spin rate, rendering these films unusable. Although WL5150 diluted with 10 vol% mesitylene does not show striations and the PPS thickness is reduced by 50% compared to undiluted PPS, it did not appreciably improve the resolution over undiluted PPS (data not shown).

2.1.2. Adhesion

In our original process, the PPS adheres poorly to PDMS after microelectrodes are patterned, and often delaminates during the development step of the encapsulation process. **Figures 3**a and 3b show contact holes of identically processed samples without and with PPS delamination, respectively. PPS adheres well to plasma oxidized PDMS without microelectrodes (Figure 3c). Thus, the process of patterning microelectrodes on PDMS is likely the reason for the weakened adhesion between the PDMS substrate and the PPS, which is applied after metal patterning. We first identify the cause for the weakening of the adhesion, and then describe remedies.

2.1.2.1. Root Cause Analysis for PPS Delamination. The metal patterning process includes lithography, metal etch, and resist strip, and exposes the PDMS surface to three solutions: I) the photoresist (PR) developer (AZ312MIF, Clariant), II) the chromium etchant CR7 ($Ce^{IV}(NH_4)_2(NO_3)_6$, $KClO_4$ in H_2O, Cyantek), and III) the gold etchant GE6 (KI, I_2 in H_2O, Transene). To examine which interaction causes the weakening of the adhesion, PDMS

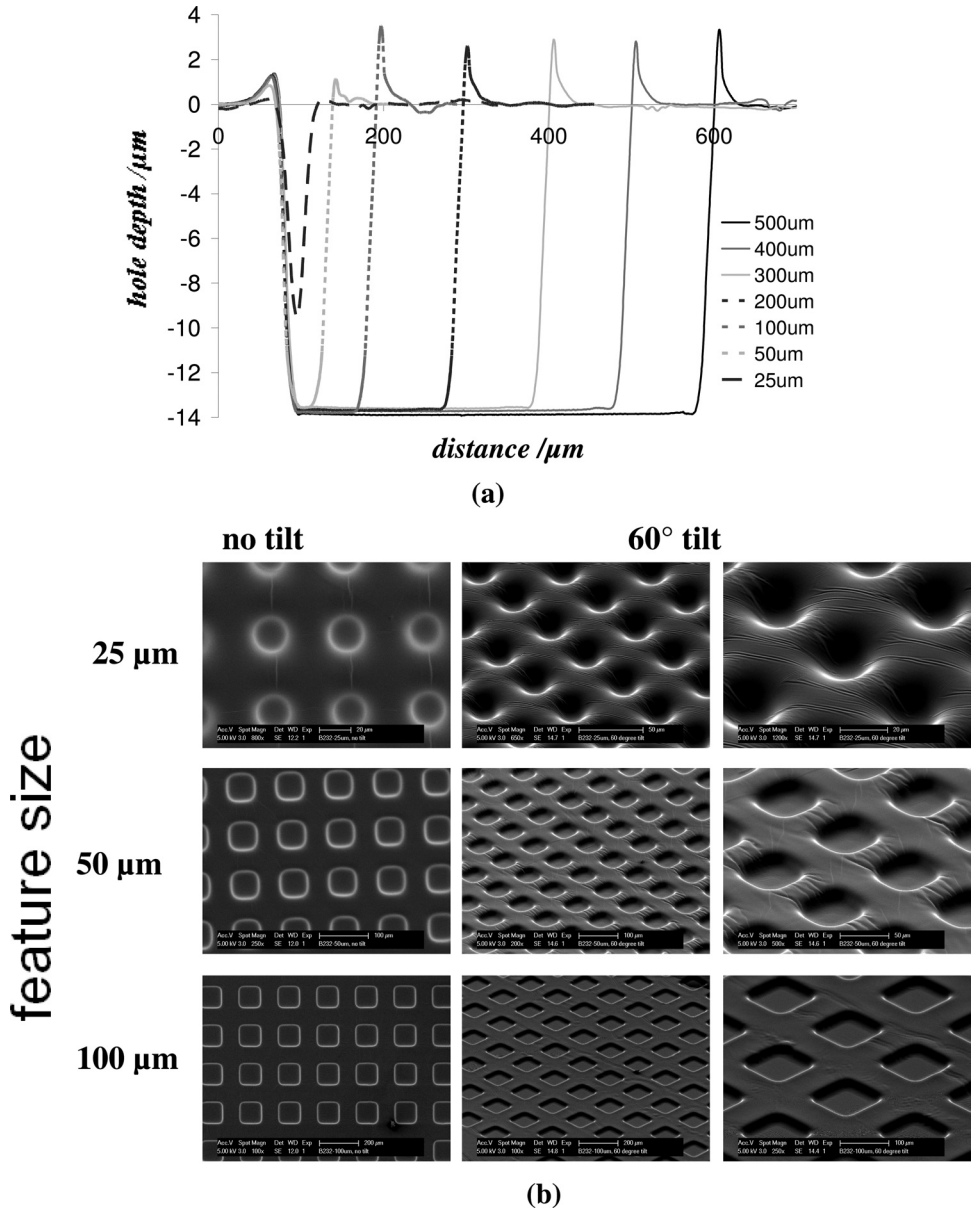

Figure 2. a) Profilometer scans of 25–500 µm wide square contact holes in PPS (the "spike" on the right side of each contact hole is an artifact of the measurement, caused by the stylus pushing against the soft wall of the contact hole[35]), and b) SEM images of 25 µm, 50 µm, and 100 µm wide contact holes with and without tilt of the sample.

membranes without microelectrodes were immersed separately in one of each solution, before PPS was spun on. The duration of the immersion was chosen to considerably exceed the typical duration employed for patterning microelectrodes on SMEAs. Immersing the PDMS for 600 s in CR7 solution (Figure 3d) or for 1200 s in the PR developer (Figure 3e) did not appreciably affect the adhesion of the PPS. However, immersing the PDMS in GE6 solution for 600 s (Figure 3f) caused complete PPS delamination. The PDMS also takes on a faint yellow color which indicated that it absorbed iodine. When the PDMS is immersed for only 15 s in GE6 the PPS partially delaminates (Figure 3g), and leaves a pattern that is very similar to the delamination pattern that is often observed during the encapsulation of SMEAs (Figure 3b). These findings strongly suggest that the interaction of the iodine in the etchant with the PDMS causes the adhesion to the PPS to weaken.

2.1.2.2. Remedies Against PPS Delamination. We explored three remedies against PPS delamination from the PDMS.

Chemical reduction of iodine: Gold is a noble metal and therefore requires an etchant with high oxidation potential. Etching with GE6 is a very efficient yet gentle method to pattern gold films. Most other gold etchants, such as aqua regia, would also oxidize the PDMS and/or the PR. We therefore opted to minimize the detrimental effect of the GE6 etchant on PPS adhesion rather than to change the etchant. To minimize

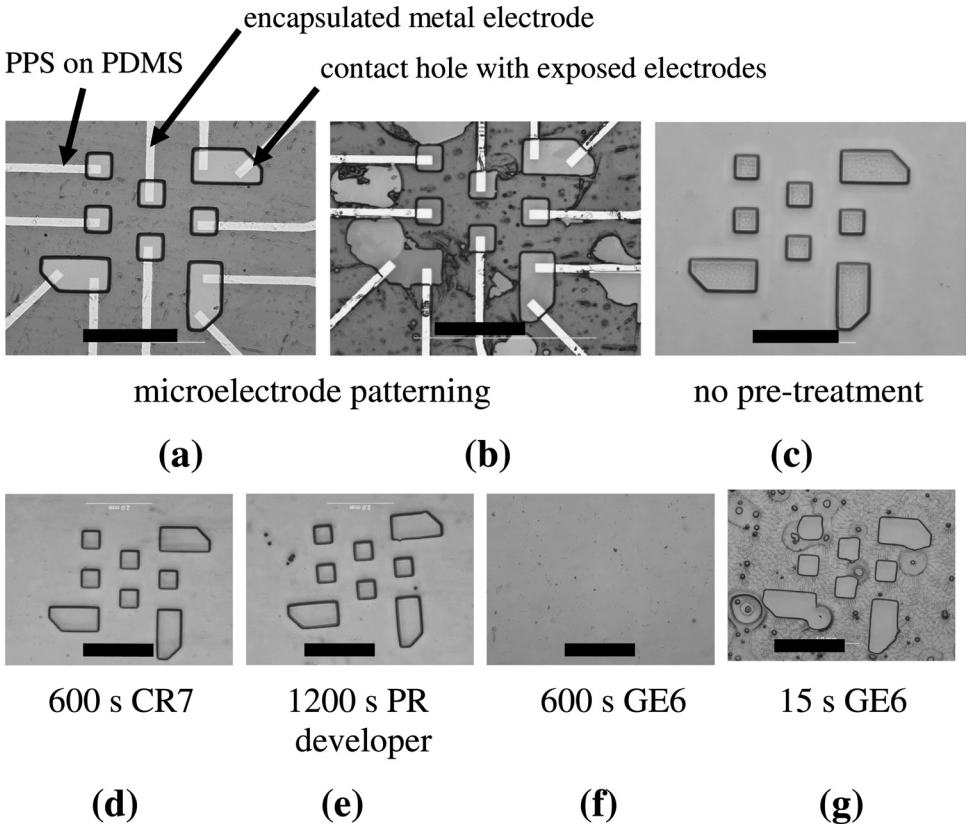

Figure 3. Optical microscopy images of PPS patterned on PDMS; a,b) with microelectrodes – a) without, and b) with delamination, and c–g) without microelectrodes – c) no pre-treatment, d) 600 s in CR7, e) 1200 s in PR developer, f) 600 s in GE6, and g) 15 s in GE6. Scale bar: 1 mm.

exposure to GE6, the sample is taken out of the solution as soon as the gold is etched (no over-etching). The sample is immersed in a 0.1 M solution of sodium thiosulfate immediately after etching. The thiosulfate chemically reduces to iodide the iodine that remains on and in the PDMS: $I_2 + 2S_2O_3^{2-} \rightarrow 2I^- + S_4O_4^{2-}$. We found that a 30 s immersion of the sample in the thiosulfate solution results in the best adhesion. In nearly all instances this procedure prevented the delamination of the PPS from the PDMS substrate. A shorter immersion does not provide adequate iodine reduction, and prolonged immersion did not improve the adhesion, but had the opposite effect. We have not observed any detrimental effects of this treatment on the capability of the SMEA to record/stimulate neural activity.

Deposition of an adhesion layer: Coating the PDMS surface with a layer of 1–2 nm Cr or Ti after gold etching and before PPS application greatly improves the adhesion to the PDMS. Cr or Ti layers of such thickness on PDMS are discontinuous and do not conduct electrically.

Reduction of mechanical force: Weak adhesion causes the PPS to delaminate from the PDMS. Using an air brush instead of a shower rinse for the development of the PPS reduces the mechanical force. The contact holes that can be produced with the air brush process are slightly larger than what can be achieved with the IPA shower rinse, however, the air brush provides an improved process window against delamination.

A combination of these remedies largely eliminated PPS delamination during SMEA fabrication.

2.1.3. Resolution of Patterning PPS on PDMS with Microelectrodes

To demonstrate the resolution of the PPS on the target device, we fabricated SMEAs with different contact hole sizes on the same substrate. The sizes of the contact holes were 25 µm, 40 µm, 50 µm, 60 µm, 75 µm, and 100 µm. **Figure 4**a–c shows 100 µm, 75 µm and 50 µm wide square contact holes to metal electrodes. Holes were opened with an air brush (Figure 4a) or a shower rinse (Figure 4b and 4c). Comparing the resolution of the patterning process with an air brush and with a shower rinse, both using a 40 s mesitylene soak, confirms the resolution obtained on bare PDMS (Section 2.1.1). 50 µm contact holes can be patterned with the shower rinse, and 75 µm contact holes can be patterned using the air brush.

The shower rinse process coupled with an 80 s mesitylene soak gave the best resolution on PDMS without microelectrodes. However, when this longer mesitylene soak is used on PDMS with patterned microelectrodes, the PPS delaminates in most cases, even when all the precautions described in the preceding section were employed. This demonstrates that the remedies do not completely recover the adhesion of the PPS to a level that is comparable to untreated PDMS. This process therefore can not be used to fabricate SMEAs.

Figure 4d,e show the contact holes to microelectrodes that were patterned with a 40 µm and 25 µm square mask, respectively, using the optimized process. In the 40 µm contact hole, the foot in the encapsulating silicone layer is clearly visible and

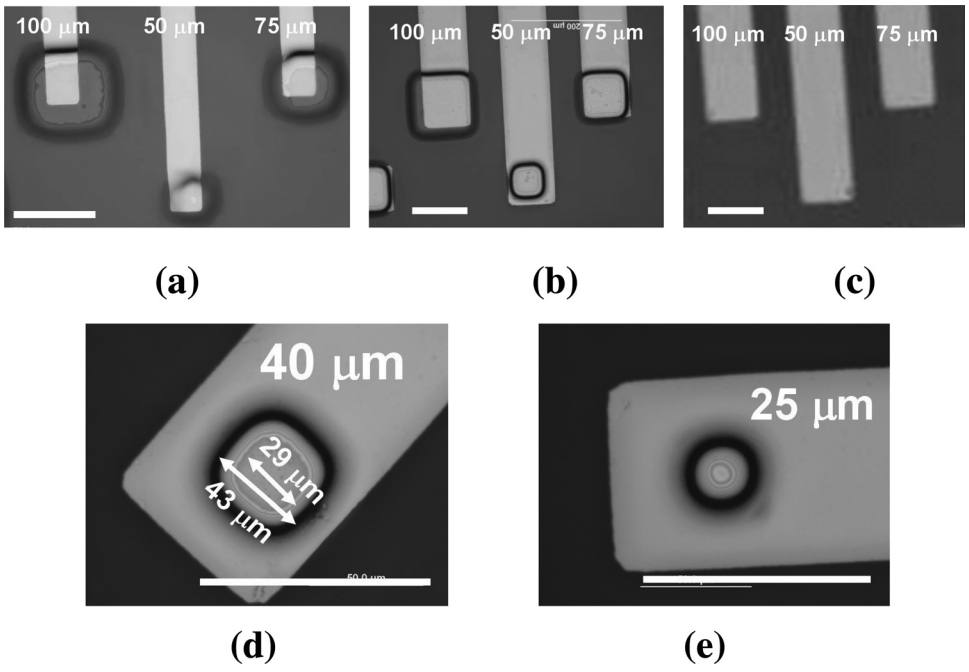

Figure 4. Recording sites of microelectrodes encapsulated with PPS using different development processes: a) 40 s mesitylene, air brush, b,d,e) 40 s mesitylene, shower rinse, and c) 80 s mesitylene, shower rinse (no encapsulation layer left due to delamination). Scale bar: 100 μm.

extends 6–7 μm from the edge of the mask. The contact hole in the encapsulation is therefore only about 29 μm in diameter. The PPS in the 25 μm contact hole is not completely removed, i.e., the microelectrode underneath this contact hole is electrically insulated. Impedance measurements confirm these results (data not shown). This process can therefore be used to pattern 40 μm, but not 25 μm contact holes.

2.2. Stretchable Microelectrode Arrays (SMEAs)

An SMEA with 28 microelectrodes and 100 μm contact holes was fabricated with the new encapsulation process described in Section 2.1. The size of the contact holes was chosen to be 100 μm to enable reliable, high yield fabrication, and because commercially available rigid MEAs are available with this size electrodes. We first describe the fabrication and characterization of these SMEAs. We then demonstrate the application of these SMEAs to record and stimulate neural activity from a hippocampal tissue slice when the SMEA is stretched equibiaxially (tissue is not stretched appreciably). Finally, we show that these SMEAs are also biocompatible for at least two weeks in vitro.

2.2.1. Fabrication of SMEAs and Assembly

A detailed description for fabricating the new, higher resolution SMEA is provided in the experimental section. After fabrication, the SMEA with 28 microelectrodes and 2 reference electrodes is removed from the glass slide and sandwiched between two printed circuit boards (PCBs) with circular openings in their centers (**Figure 5**a). Contact pads on the upper PCB allow the pins of an amplifier to make electrical contact to the microelectrode underneath. The microelectrodes are then electroplated with platinum black to reduce their impedance, hence the noise of the recording. Figure 5b shows the recording sites of the microelectrodes after electroplating. The microelectrode impedance at 1 kHz is reduced from ~2–4 MΩ before to ~100 kΩ after electroplating (see Supporting Information).

2.2.2. Recording and Stimulating Neural Activity in a Hippocampal Tissue Slice with Equibiaxially Stretched Microelectrodes

We demonstrated the capability of the SMEA to record and stimulate neural activity from hippocampal tissue slices over one complete cycle of stretching and relaxation, i.e., before, during, and after stretching the SMEA. **Figure 6** shows details

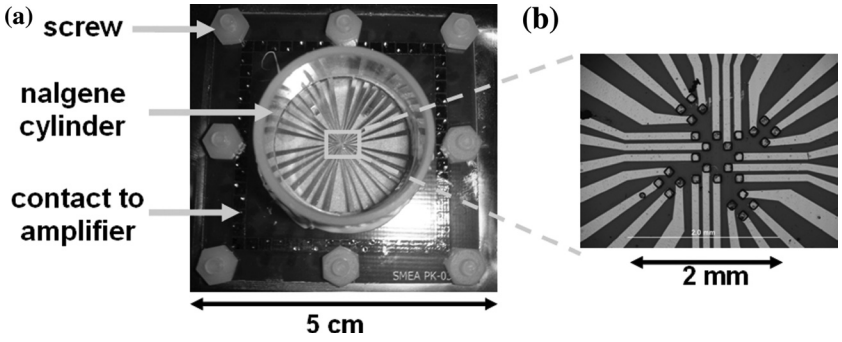

Figure 5. a) SMEA with 28 microelectrodes and two reference electrodes sandwiched between two printed circuit boards and with a plastic cylinder attached to form a growth well, and b) optical microscopy image of the recording sites after electroplating.

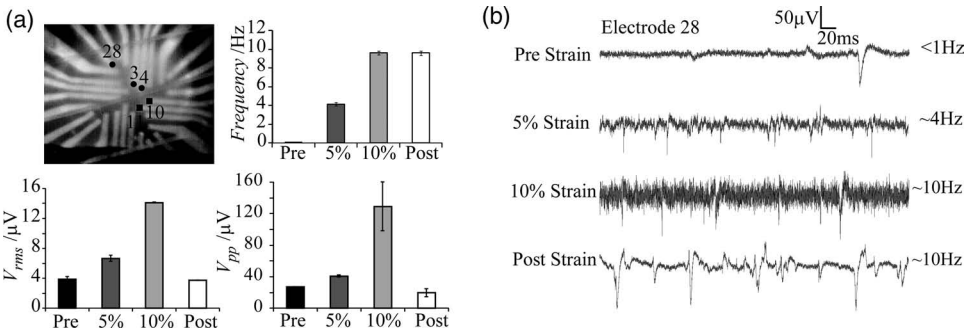

Figure 6. a) Photograph of an organotypic hippocampal tissue slice on the SMEA. Recording electrodes are indicated by circles with the electrode number indicated. Stimulating electrodes are indicated by squares. Frequency of spontaneous activity, V_{rms}, and V_{pp} before stretching (Pre), at 5% and at 10% equibiaxial strain, and after relaxation (Post); b) Representative traces of spontaneous activity recorded on electrode 28 before stretching (Pre), at 5% and at 10% equibiaxial strain, and after relaxation (Post). The frequency of spontaneous activity is indicated.

of the spontaneous activity recorded from the hippocampal tissue slice. The upper left corner of Figure 6a shows a higher-magnification optical micrograph of the recording area of the SMEA and the hippocampal tissue slice. The microelectrodes are numbered clockwise. The other three corners of Figure 6a show the root-mean-square voltage (V_{rms}), the peak-to-peak voltage (V_{pp}) and the frequency of spontaneous neural activity as recorded from electrode 28 before stretching (Pre), at 5% and at 10% equibiaxial strain, and after relaxation (Post). Figure 6b shows the corresponding representative recording traces in the different states.

V_{rms} and V_{pp}, i.e., the noise of the recording, both increase with increasing strain in the SMEA. V_{rms} and V_{pp} increase because the impedance of the microelectrodes increases when strained.[10] Upon relaxation (Post), the impedance, hence V_{rms} and V_{pp}, decreases to the level before stretching (Pre), indicating that the SMEA is elastically stretchable. The frequency of spontaneous neural activity increases with strain, and remains high after relaxation.

Figure 7 shows the evoked activity of hippocampal tissue slices, at strains of 0% before stretching, at 5% and 10% equibiaxial strain, and again at 0% strain post-stretch. Figure 7a shows representative evoked responses and the quality of the recorded signal. The biphasic stimulating pulse is given through electrodes 10 and 11; the recordings shown are from electrodes 3 and 4. The stimulating pulse from the microelectrodes is capable of evoking activity from the tissue before, during, and after stretching. The noise of the evoked recordings increases with increasing strain, and returns to pre-stretch levels after relaxation. This is equivalent to the behavior observed for spontaneous activity.

Figure 7b shows the stimulus/response (SR) curves obtained for the stimulation of the tissue for different strains of the SMEA (the tissue did not stretch appreciably). The SR curves show the magnitude of the evoked response (in μV) for different stimulus intensities (in μA). Before stretching (Pre-strain), the SR curve shows the typical sigmoidal relationship.[36] At low stimulus intensities, the evoked responses are small. With increasing stimulus intensity, the magnitude of the evoked response increases, and reaches a plateau when essentially all available neurons are excited. At 5% strain, the SR curve retains the sigmoidal shape, but the maximum evoked response is reached at a stimulating current of ~100 μA compared to ~130 μA before stretching. At 10% strain, the recordings are very noisy, thus determination of the magnitude of the evoked response is challenging. In addition, the increased electrode resistance leads to an increased stimulus artifact which has a tendency to saturate the amplifiers. After relaxation, the quality of the recordings improves as the electrode impedance returns to pre-stretch values. The SR curve regains the sigmoidal shape with a maximum evoked response at ~60 μA stimulating current.

2.2.3. Biocompatibility Studies

To evaluate the biocompatibility, hippocampal tissue slices were cultured for two weeks on an SMEA. The slices were then treated with propidium-iodide (PI) which is a fluorescent indicator of dead cells. The cultures show a well-preserved morphology of the hippocampus with very little PI staining, indicating very few dead cells (see Supporting Information).

3. Discussion

The research we report here provides solutions for two important issues for applications in stretchable electronics in general, and to neural interfaces specifically: resolution of patterning contact holes and adhesion of the encapsulation layer to the PDMS substrate.

According to product specifications, features of <15 μm width can be patterned with the PPS WL5150, and even 10 μm feature sizes have been reported.[30] In practice, the realized minimum feature sizes for applications in stretchable neural interfaces are much larger. There are two main reasons for the discrepancy in specified and achieved resolution. i) *The substrate*: WL5150 was developed for packaging applications in the semiconductor industry to alleviate the thermal stress between the PCB and the die.[33] It is also used in bioMEMS applications.[30,37,38] In these applications, silicon or silicon dioxide are the typical substrates. In neural interface and stretchable electronics applications, the substrate is PDMS. The adhesion between WL5150 and PDMS is weaker, particularly after the patterning of microelectrodes, than the adhesion between WL5150 and SiO_2.

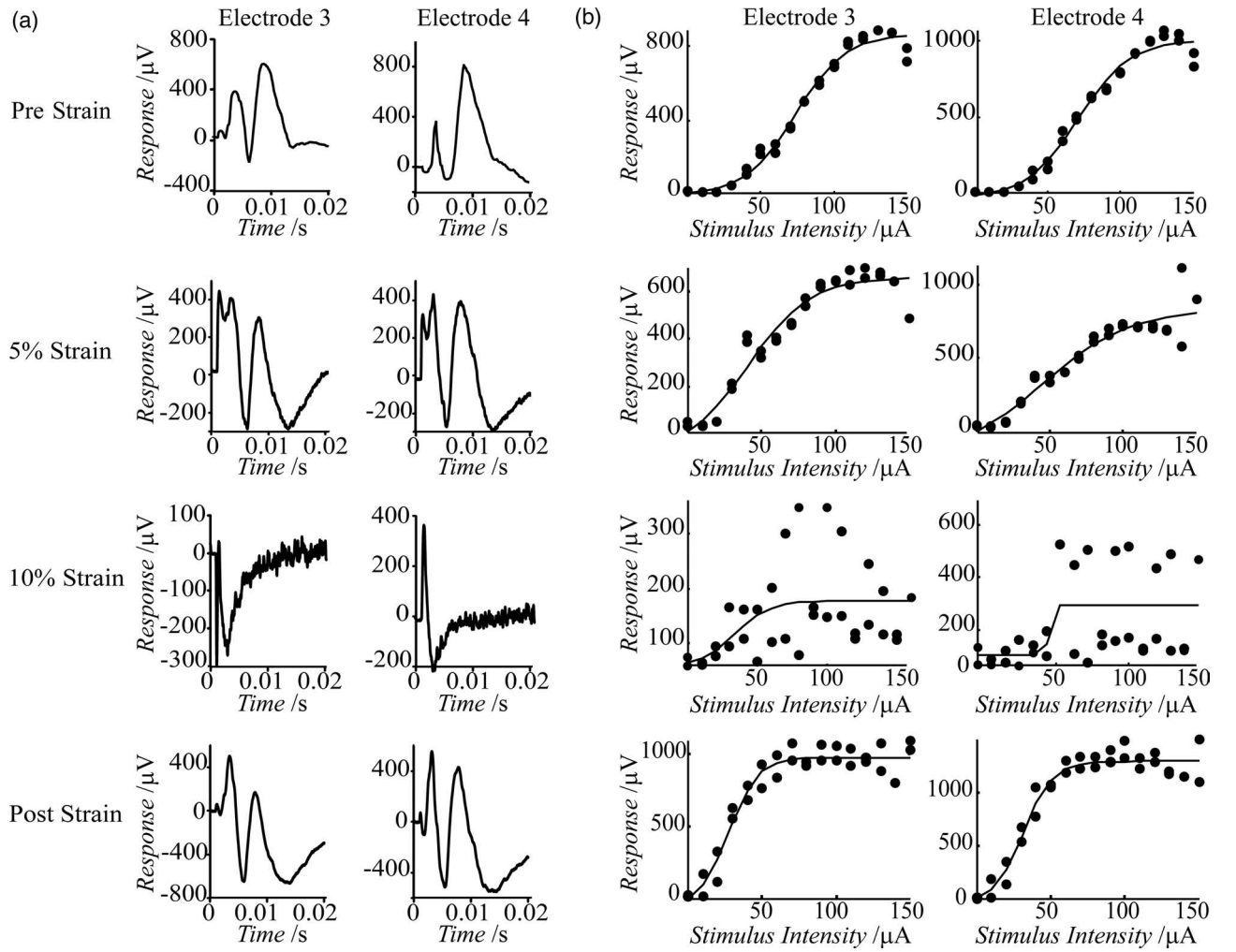

Figure 7. a) Maximum evoked responses during stimulus-response measurements, and b) stimulus-response curves, both at strains of 0% before stretching, at 5%, 10%, and again at 0% strain post stretch conditions, from electrodes 3 and 4.

Therefore, a development process that uses shorter mesitylene soak and IPA rinse with less force is necessary to avoid delamination of the WL5150 from the PDMS, causing the resolution to deteriorate. ii) *The features*: The nature of the patterned features is different for packaging or bioMEMS applications than for neural interfaces applications. Whereas silicone mesas are patterned in packaging applications, contact holes are patterned in neural interface applications. In the former case, most of the WL5150 is removed during the development process leaving silicone pillars behind. In the latter case, most of the WL5150 remains on the substrate and small contact holes are formed. For a given PPS thickness, complete removal of the WL5150 becomes increasingly difficult with decreasing hole size. On the other hand, removal of the WL5150 does not necessarily become more difficult for mesas of smaller dimensions. For both of these reasons, substrate and the nature of the features, the resolution of the WL5150 is often lower for neural interface applications than for packaging applications.

In neural interface applications, the recessed electrode must be cleared of electrically insulating PPS residues inside the contact hole. If the metal electrode at the bottom of a contact hole is covered with residues of PPS, electrical contact to the tissue can not be established and electrical signals from the tissue can not be recorded. The resolution of the patterning process is limited by the slope of the sidewall and the formation of the "foot" at the bottom of the contact hole. The "foot" is caused by activation of the catalyst in the WL5150 in the unexposed areas of the sample. This activation may be induced thermally during hard bake, or photochemically by light scattering during exposure. For optimum resolution, thermal and photochemical activation of the catalyst in unexposed regions must be minimized.

To photopattern PPS at high resolution, thermal activation of the catalyst during the thermal treatment steps needs to be minimized. On the other hand, the PPS must be sufficiently crosslinked to provide mechanical stability and to prevent delamination of the encapsulation layer during the development process. The hard bake step therefore needs to be long enough to ensure adequate crosslinking but short enough not to significantly impact the resolution. Our results demonstrate that 120 s is the optimum

hard bake duration. A longer hard bake causes thermal activation of the catalyst inside the contact hole, while a shorter hard bake does not provide sufficient crosslinking. The optimized hard bake time depends on the thickness of the PDMS and on the thickness and the thermal conductivity of the backing plate.

For high resolution patterning, photochemical catalyst activation in the unexposed areas due to scattering of photons needs to be minimized. This can be realized with the following approaches. i) *Avoid reflection of photons from the mask aligner sample tray*: The reflection of photons can be minimized by either coating the glass backing plate with an opaque film or covering the sample tray with a black sheet. This is not necessary if a backing plate made of an opaque material is used. ii) *Avoid over- and underexposure*: Increasing the exposure time beyond 240 s does not increase the PPS thickness after development, indicating complete catalyst activation. Much longer exposure times increase the size of the foot, thus, reduce the resolution of the process. An exposure time of less than 240 s causes the PPS thickness to be lower because not all of the catalyst is activated, resulting in incomplete crosslinking which contributes to delamination. To account for sample-to-sample variation, an exposure time of 300 s was chosen for the fabrication of SMEAs. iii) *Bring sample close to mask*: The sample can not be brought into physical contact with the mask during exposure because the tacky PPS sticks to the mask and easily delaminates from the underlying PDMS upon removal. Increasing the soft bake time reduces the tackiness of the PPS, but not enough to eliminate delamination after contact with the mask. Covering the sample with Mylar foil during exposure reduces the delamination, but does not eliminate it. Bringing the sample close to the mask without actually touching it minimizes the photochemical activation of the catalyst by photons arriving at an oblique angle at the sample.

During the development process, a mechanical force is required for high resolution patterning to clear the contact holes from PPS residues. On the other hand, the larger the mechanical force is, the higher the possibility for delamination. Using an air brush instead of a shower head reduces the mechanical force on the PPS, thus delamination. However, the resolution of the patterning process deteriorates from 50 μm contacts holes that can be produced using a shower rinse to 75 μm contact holes employing an air brush.

The resolution of the encapsulation process is largely unaffected by the PPS thickness. Dilution of the PPS with mesitylene produces thinner films, however, the minimum size of the contact holes remains the same. This suggests that the "foot" at the bottom of the contact holes, and not the sidewall slope, is the main factor that limits the resolution.

PPS adheres strongly to many substrates, such as glass, SiO_2, and even plasma oxidized PDMS (without microelectrodes). However, when a gold film is first deposited and patterned lithographically on the PDMS to create microelectrodes, the adhesion of PPS is compromised, and it delaminates frequently during the development process. This delamination must be avoided to prevent shunts between the electrodes. The extent of delamination varies from small areas to the whole surface.

We identified absorption by the PDMS of the iodine in the gold etchant as the cause for the deterioration of the PPS adhesion. The adhesion can be improved to a level sufficient for the fabrication of SMEAs by immersion of the sample after etching in thiosulfate solution, deposition of a 1–2 nm thick (therefore non-conducting) layer of Cr or Ti, and, if 75 μm or larger contact holes are required, use of an air brush for the development. However, the adhesion can not be recovered to the same level as on pristine PDMS. This is illustrated by the fact that the PPS delaminates from PDMS with patterned microelectrodes when a long (80 s) mesitylene soak is used for the development process, whereas it does not delaminate from PDMS without microelectrodes.

The SMEA consists of three materials: PDMS, PPS, and gold. PDMS and PPS have similar chemical composition but different mechanical properties. The maximum elastic elongation of PDMS and PPS are >140% and 37.6%, and the Young's moduli are 2 MPa and 160 MPa, respectively.[39] The Young's modulus of gold is 79 GPa, and thin gold films (250–2000 nm) on the polymer polyimide fracture and lose electrical conduction at strains <1%.[40] However, stretching a composite of a thin gold layer (38 nm) sandwiched between PDMS (300 μm) and PPS (<15 μm) does not result in appreciable delamination or fracture of the gold or the PPS up to strains of at least 80%. The gold remains electrically conducting provided the film has a microcracked morphology.[9] A gold film on PDMS that is not microcracked fractures and loses electrical conduction at strains <2%. Microcracked films are obtained at low deposition temperatures (<65 °C), gold thickness of 20–120 nm, and Cr or Ti adhesion layer thickness of less than 6–8 nm.[41]

The optimized process is capable of patterning 40 μm contact holes while providing adequate adhesion for the PPS. Layer-to-layer registration has not been an issue because the recording characteristics of the microelectrodes are not strongly affected by small misalignments. We fabricated SMEAs with 28 microelectrodes and 100 μm contact holes to demonstrate their capability to record and stimulate neural activity, even while the SMEA was mechanically strained. We recorded the spontaneous and evoked activity of a hippocampal tissue slice before stretching, at 5% and 10% equibiaxial strain, and after relaxation. The frequency of the spontaneous neural activity and the noise of the recording both increase with strain. After relaxation, the noise of the recording returns to pre-stretch level whereas the frequency of the neural activity remains elevated for up to 30 min.[6] The observed increase in the frequency of neural activity after the SMEA was stretched may be caused by an irritation of the tissue due to shearing along the SMEA underneath. At 10% equibiaxial strain, the SMEA remains functional for the recording of spontaneous activity. However, the noise of the recording is high, and only neural activity with high amplitude can be observed. The SMEA demonstrated good biocompatibility making possible long term studies.

These results illustrate that SMEAs with dimensions and number of microelectrodes similar to those of commercial MEAs on glass or flexible MEAs on polyimide can be fabricated.

4. Conclusions

Our findings illustrate a new and improved fabrication process of elastically stretchable neural interfaces. We demonstrate that these SMEAs are capable of recording and stimulating neural

activity in hippocampal tissue slices when stretched equibiaxially up to at least 5%. In previous generations of SMEAs, the number of microelectrodes was limited by the resolution of the encapsulation process. In this article, we have demonstrated how improvements in the resolution of the encapsulation layer allow us to increase the number of microelectrodes on the SMEA from 11 to 28 while maintaining the ability to record neural signals. This increase in the number of microelectrodes is accompanied by a reduction in the minimum feature size in the encapsulation layer from 300 μm × 300 μm (equal to 90 000 μm^2) to 100 μm × 100 μm (equal to 10 000 μm^2). We also demonstrate the feasibility of patterning 40 μm × 40 μm (equal to 1 600 μm^2) features, which will allow a further increase in the number of microelectrodes in future generations of SMEAs. Smaller contact holes in the encapsulation layer allow the microelectrodes to interface with a smaller neural population.

Importantly, this new fabrication process also greatly increases the adhesion of the encapsulation layer in SMEAs to the underlying PDMS after microelectrodes are patterned on it. The delamination of the encapsulation layer severely limited the yield of SMEA fabrication in the past. We describe experiments to determine the cause of poor adhesion, and demonstrate which remedies are suitable to increase adhesion. Implementation of these remedies greatly increases the fabrication yield for SMEAs.

In sum, our improved encapsulation process has several advantages over extant methods. These will contribute to the future development of neural interfaces for in vitro and in vivo biomedical applications that involve the recording and stimulation of neural activity.

5. Experimental Section

Fabrication of Microelectrode Arrays: A glass slide was coated with a monolayer of perfluorooctyl-tricholorsilane (Sigma Aldrich) to facilitate the removal of the silicone membrane at the end of fabrication. The PDMS membrane (Sylgard184, Dow Corning) was prepared using standard methods.[10]

A film of 3 nm of Cr or Ti and 38 nm of Au was deposited on the PDMS substrate by electron beam evaporation (DV-502A, Denton). The pattern for the microelectrodes was created by spinning on the photoresist (AZ5214, Clariant), exposure (MJB3, Karl Suss) through a photomask and development. The exposed gold layer was etched with GE6 solution, and immersed in a solution of sodiumthiosulfate pentahydrate (0.1 M, Sigma-Aldrich) for 30 s. To remove the bottom chromium layer, the sample was dipped briefly in CR7 etch. The resist was stripped by UV exposure for 10 min and soak in AZ312MIF developer.

A 1–2 nm thick layer of Cr or Ti was deposited on the sample by electron-beam evaporation. The encapsulation process is carried out as described in section 2. The air brush (Badger Airbrush Co, Model 200) pressure is estimated to be 30 psi (inlet air pressure: 60 psi).

Dilution Experiments: For a 10, 25, and 50 vol% dilution, 10 mL of the solution were comprised of 9, 7.5, and 5 mL WL5150 and 1, 2.5, and 5 mL of mesitylene, respectively.

Thickness and Residue Measurements: The thickness of the WL5150 was measured with a profilometer (P-15 surface profiler, KLA Tencor), using a downward force of 1 mg. The residue in the contact holes was calculated as the difference between the thickness of the PPS of typically 14–15 μm next to the largest openings and the depth of a given contact hole. A residue of 0 μm means that the depth of the contact hole equals the thickness of the PPS, i.e., a microelectrode in the contact hole would not be electrically insulated. The error bars in Figure 1 indicate the maximum and the minimum residue measured (i.e. the range of residue) for a given hole size for at least three measured holes. The generally larger error bars for larger contact holes reflect a higher variability in the depth of the contact hole, i.e., the amount of residue inside the contact hole. For thickness measurements in the exposure dose experiment, a glass substrate was used to accurately measure the PPS thickness.

Assembly: The SMEA was sandwiched between two PCBs which were held together by nylon screws (Digi-Key, Figure 5a). Silver paste (Epoxy Technology) on the contact pads of the microelectrodes facilitated the electrical contact to the PCB. A plastic cylinder (Nalgene, Thermo Fisher Scientific) with a diameter slightly larger than that of the openings in the PCBs was attached with epoxy adhesive (Tra-Bond BA-FDA2, Tra-Con) to the upper PCB to form a culture well.

Electroplating: The culture well was filled with the electroplating solution (5.27 g $H_2[PtCl_6]$·aq, Sigma-Aldrich, and 71.4 mg lead acetate, Sigma-Aldrich, dissolved in 350 mL de-ionized water), and a Pt counter electrode (anode) was suspended in it. The microelectrodes were the (grounded) cathode. The electroplating was carried out at a constant current (261 Picoampere Source, Keithley Instruments) of 1.2 μA for 60 s (current density: 40 mA/cm^2). The plating solution was agitated with ultrasound during electroplating to shake off loosely adhering platinum from the underlying gold. After plating, the SMEA was soaked in de-ionized water for at least 24 h to wash out adsorbed lead.

Impedance Measurement of the Microelectrodes: The impedance was measured (HP 4274A Multi Frequency LCR meter) at 100 mV and at frequencies ranging from 100 Hz to 100 kHz against a Pt counter electrode that is dipped into a phosphate buffered saline (PBS) solution that filled the culture well. The impedance at 1 kHz is usually used to evaluate the electrode's capability of electrophysiological recording because most neural activity occurs with roughly this frequency.

Evaluation of the Recording and Stimulation Capabilities of the SMEAs: Stimulators and amplifiers from MultiChannel Systems were used to evaluate the SMEAs. During recording, the well on the PCB contained the culture medium and a hippocampal tissue slice. The hippocampal tissue slice, which was grown on a Millipore membrane (PTFE), was prepared for recording of electrophysiological activity as described previously.[6,42] The tissue is sandwiched between the Millipore membrane above and the SMEA below. Bi-axial strain in the SMEA is generated by pushing it over a hollow cylindrical indenter with a diameter slightly smaller than that of the openings in the PCBs.[43] The induced SMEA strain is verified by image analysis of photographs taken before and during stretch.[42] Spontaneous and evoked electrophysiological activity were recorded from the hippocampal tissue slice about 5 minutes after stretching the SMEA, and SR curves were derived according to published methods.[36] To evoke activity in the tissue, a biphasic rectangular current pulse is applied through two of the microelectrodes. At one microelectrode, a positive pulse is injected for a duration of 100 μs followed by a negative pulse of 100 μs duration. The pulse sequence at the other stimulating microelectrode is 180° out of phase with the first one. The amplitude of the current pulse is increased from 0 μA to 150 μA in steps of 10 μA. The inter-stimulus interval was 10 s. For each current amplitude, three consecutive measurements of evoked activity were carried out.

Supporting Information

Supporting Information is available from the Wiley Online Library or from the author.

Acknowledgements

This research was supported by the NIH (NINDS R21 052794) and by the New Jersey Commission for Brain Injury Research (09-3209-BIR-E-2).

Received: September 26, 2011
Published online: December 8, 2011

[1] R. Pelrine, R. Kornbluh, G. Kofod, *Adv. Mater.* **2000**, *12*, 1223.
[2] S. Wagner, S. P. Lacour, J. Jones, P. I. Hsu, J. C. Sturm, T. Li, Z. Suo, *Physica E* **2004**, *25*, 326.
[3] D. P. J. Cotton, I. M. Graz, S. P. Lacour, *IEEE Sens. J.* **2009**, *9*, 2008.
[4] R. Carta, P. Jourand, B. Hermans, J. Thoné, D. Brosteaux, T. Vervust, F. Bossuyt, F. Axisa, J. Vanfleteren, R. Puers, *Sens. Act. A* **2009**, *156*, 79.
[5] S. P. Lacour, J. Jones, S. Wagner, T. Li, Z. Suo, *Proc. IEEE* **2005**, *93*, 1459.
[6] Z. Yu, O. Graudejus, C. Tsay, S. P. Lacour, S. Wagner, B. Morrison III, *J. Neurotraum.* **2009**, *26*, 1135.
[7] K. W. Meacham, R. J. Giuly, L. Guo, S. Hochman, S. P. DeWeerth, *Biomed. Microdev.* **2008**, *10*, 259.
[8] J. J. FitzGerald, S. P. Lacour, S. B. McMahon, J. W. Fawcett, *IEEE Trans Biomed. Eng.* **2009**, *56*, 1524.
[9] S. P. Lacour, D. Chan, S. Wagner, T. Li, Z. Suo, *Appl. Phys. Lett.* **2006**, *88*, 204103.
[10] O. Graudejus, Z. Yu, J. Jones, B. Morrison III, S. Wagner, *J. Electrochem. Soc.* **2009**, *156*, P85.
[11] J. Jones, S. P. Lacour, S. Wagner, Z. Suo, *J. Vac. Sci. Technol. A* **2004**, *22*, 1723.
[12] D. H. Kim, J. H. Ahn, W. M. Choi, H. S. Kim, T. H. Kim, J. Song, Y. Y. Huang, Z. Liu, C. Lu, J. A. Rogers, *Science* **2008**, *320*, 507.
[13] D. H. Kim, J. Xiao, J. Song, Y. Y. Huang, J. A. Rogers, *Adv. Mater.* **2010**, *22*, 2108.
[14] D. Brosteaux, F. Axisa, M. Gonzalez, J. Vanfleteren, *IEEE Electron Device Lett.* **2007**, *28*, 552.
[15] T. Sekitani, T. Someya, *Adv. Mater.* **2010**, *22*, 2228.
[16] L. Guo, K. W. Meacham, S. Hochman, S. P. DeWeerth, *IEEE Trans. Biomed. Eng.* **2010**, *57*, 2485.
[17] M. A. Nicolelis, D. Dimitrov, J. M. Carmena, R. Crist, G. Lehweh, J. D. Kralik, *Proc. Natl. Acad. Sci. USA* **2003**, *100*, 11041.
[18] V. S. Polikov, P. A. Tresco, W. M. Reichert, *J. Neurosci. Methods* **2005**, *148*, 1.
[19] R. Biran, D. C. Martin, P. A. Tresco, *J. Biomed. Mat. Res. A* **2007**, *82A*, 169.
[20] J. Subbaroyan, D. C. Martin, D. R. Kipke, *J. Neural Eng.* **2005**, *2*, 103.
[21] http://www.multichannelsystems.com (accessed November, 2011).
[22] M. Schuettler, S. Stiess, B. V. King, G. J. Suaning, *J. Neural Eng.* **2005**, *2*, S121.
[23] J. Garra, T. Long, J. Currie, T. Schneider, R. White, P. Paranjape, *J. Vac. Sci. Technol. A* **2002**, *20*, 975.
[24] T. Adrega, S. P. Lacour, *J. Micromech. Microeng.* **2010**, *20*, 055025.
[25] L. Guo, S. P. DeWeerth, *Adv. Mater.* **2010**, *22*, 4030.
[26] K. S. Ryu, X. Wang, K. Shaik, C. Liu, *J. Micromech. Sys.* **2004**, *13*, 568.
[27] X. Niu, S. Peng, L. Liu, W. Wen, P. Sheng, *Adv. Mater.* **2007**, *19*, 2682.
[28] M. A. McClain, I. P. Clements, R. H. Shafer, R. V. Bellamkonda, M. C. LaPlace, M. G. Allen, *Biomed. Microdevices* **2011**, *13*, 361.
[29] H. Cong, T. Pan, *Adv. Funct. Mater.* **2008**, *18*, 1912.
[30] S. P. Desai, B. M. Taff, J. Voldman, *Langmuir* **2008**, *24*, 575.
[31] D. P. J. Cotton, A. Popel, I. M. Graz, S. P. Lacour, *J. Appl. Phys.* **2011**, *109*, 054905.
[32] M. Schuettler, C. Henle, J. Ordonez, G. J. Suaning, N. H. Lovell, T. Stieglitz, *Proc. 3rd Int. IEEE EMBS Conf. Neural Eng.* **2007**, 53.
[33] B. Harkness, G. Gardner, J. Alger, M. Cummings, J. Princing, Y. Lee, H. Meynen, M. Gonzalez, B. Vandevelde, M. V. Bulcke, C. Winters, E. Beyne, *Proc. SPIE, Bellingham, WA*, **2004**, *5376*, 517.
[34] O. Graudejus, C. Tsay, S. Wagner, Z. Yu, B. Morrison III, S. Lacour, *Mat. Res. Soc. Symp. Proc. Spring Meeting*, 1009-U04-02, San Francisco, 9-13 April 2007.
[35] J. Jones, O. Graudejus, S. Wagner, *J. Electron. Mater.* **2011**, *40*, 1335–1344.
[36] Z. Yu, B. Morrison III, *J. Neurophysiol.* **2010**, *103*, 499.
[37] S. L. Peterson, A. McDonald, P. L. Gourley, D. Y. Sasaki, *J. Biomed. Mater. Res., Part A* **2005**, *72*, 10.
[38] J. N. Lee, X. Jiang, D. Ryan, G. M. Whitesides, *Langmuir* **2004**, *20*, 11684.
[39] http://www.dowcorning.com (accessed November, 2011).
[40] S. L. Chiu, J. Leu, P. S. Ho, *J. Appl. Phys.* **1994**, *76*, 5136.
[41] O. Graudejus, P. Goerrn, S. Wagner, *Appl. Mat. Int.* **2010**, *2*, 1927.
[42] B. Morrison III, H. L Cater, C. D. Benham, L. E. Sundstrom, *J. Neurosci. Meth.* **2006**, *150*, 192.
[43] H. L. Cater, L. E. Sundstrom, B. Morrison III, *J. Biomech.* **2006**, *39*, 2810.